

## Vehicle Segmentation Using Evidential Reasoning

Joon-Woong Lee\* and In-So Kweon\*\*

\* KIA Technical Center, KIA Motors,  
781-1 Sohadong Kwangmyung-Shi Kyungki-Do, Korea.

\*\* Dept. of Automation and Design Eng., KAIST  
207-43 Cheongryangridong Dondaemoongu, Seoul, Korea.

**Abstract**-This paper proposes a segmentation algorithm by means of an evidential reasoning to segment moving vehicles in front of the moving our car in a road traffic scene. Generally, an evidential reasoning finds the perceptually known evidences of a target and updates a probabilistic expectation for the target to be in an image. Since a noise image produces unreliable features and degrades the detection and localization, selecting image primitives which are less sensitive to noise and well represent the evidences is important. We carry out this task by the probabilistic integration of image features based on *maximum a posteriori*(MAP) probability that combines the prior and likelihood probabilities using Bayes' rule.

### 1: Introduction

In this paper, we are interested in monocular gray-level visual sensing for segmenting moving vehicles in front of the moving our car in a road traffic scene. The segmentation is carried out by evidential reasoning based on the probabilistic integration of low-level image features. Recently, many researchers have been working on the analysis of the road traffic scene since the late 1980's in accordance with the increasing interest about road traffic safety and intelligent vehicle development [1,2,4]. However, most previous researches have shown their feasibility in very limited environments and provided poor estimates due to noisy sources resulting from variable illumination, dynamic state, the diversity and complexity of scenes [1, 2, 3, 4]. What is worse, since the viewer moves in a dynamic road scene, it is difficult to extract only the regions corresponding to moving vehicles using familiar methods of motion segmentation[2]. These problems have made the visual perception of outdoor road environment difficult and challenging topic of computer vision.

Evidential reasoning is a method for combining

information from different sources of evidence to update probabilistic expectations. Combining of evidences thus can be quantitatively described by combining of probabilistic expectations of many sources of information, including a color, a texture, a shape and a prior knowledge in a flexible way to achieve recognition. Xie *et al.* [4] have applied a perceptual organization to extract road vehicles in a dynamic traffic environment. They considered the evidence for a road vehicle as a cluster of nearly vertical and nearly horizontal line segments, which make neighbors each other. This evidence, however, is not well consistent with various kinds of roads. Furthermore, the vertical line segments are rarely extracted on a vehicle. It means that the selection of evidences of a target is more important than the application of evidential reasoning. Using some appearance properties of the object of interest in an image, we determine evidences and search for features which satisfy the evidences. While this method provides good results in noisy environments, it is domain specific.

We determine the evidences for a leading vehicle within a driver's view such as: first, there is a sharp intensity change at the boundary of a vehicle; second, a vehicle has symmetric property. For the segmentation, we take into account the following reasonable assumptions: I) A vehicle lies on a traffic road. II) Optical axis of a CCD camera is parallel to the ground plane of a road. III) The intensity distribution with respect to road and sky is sufficiently homogeneous between two successive images. IV) The intensity distribution between a road and a vehicle is not similar. We also limit the problem by considering the following two practical constraints: I) The entire shape of the leading vehicle in front of a viewer is contained in an image. II) The road should be seen in an image.

## 2: Moving Vehicle Segmentation

Segmentation is carried out by following steps. First, we perform an image subtraction-based exclusive-or(XOR) operation to distinguish between road surface and vehicles and determine the validation region considered to minimum variation of intensity distribution of the vehicle of interest using the result. Second, we search for the symmetry axes based on the fact that the rear viewed imagery of most vehicles on a normal road possesses a symmetric property. We use the approach proposed by Zielke *et al.* [5] to find a potential symmetry axis. However, the usage of the mean intensity profile of a validation region and finding local maxima, which take advantage of MAP(*maximum a posteriori*)-based probabilistic inference to choose relevant axes, are different points from their method. Third, the outmost lines of a vehicle are extracted using the integration of visual information such as the detected symmetric axis and the three kinds of local maxima which are composed of the gradient of cumulative XOR signal, the cumulative vertical edge component and the gradient of mean intensity profile in a validation region.

### 2.1 Extracting Baseline

We carry out an XOR operation for two images  $Z_1(x, y)$  and  $Z_2(x, y)$  to isolate an image into three regions which are a region  $R_r$  dominated by road, a region  $R_s$  dominated by sky and the remainder  $R_v$ . The XOR operation, introducing a threshold  $\tau$  for equality, against all pairs of pixels at same position between  $Z_1(x, y)$  and  $Z_2(x, y)$  is expressed as

$$O(i, j) = \begin{cases} 1, & \text{if } |Z_1(i, j) - Z_2(i, j)| \leq \tau \\ 0, & \text{otherwise} \end{cases} \quad (1)$$

where  $(i, j)$  is a column and a row position on an image.

We obtain the sum of XOR signal for each row as  $S_j = \sum_i O(i, j)$  and define a parameter  $\alpha$  as

$$\alpha = \mu_e + \lambda_e \sigma_e \quad \text{where} \quad \mu_e = \sum_j S_j / N,$$

$\sigma_e^2 = \sum_j (S_j - \mu)^2 / (N - 1)$ , in which  $N$  is the number of column pixels, and  $\lambda_e$  is the Gaussian coefficient defined in Gaussian distribution table. The  $\alpha$  divides the sum of XOR signal into sparse part and dense part. There

are two baselines: One of them is  $H_s$  which splits  $R_s$  and  $R_v$ . The other is  $H_r$  which partitions  $R_r$  and  $R_v$ .

Fig. 1 shows an example of XOR operation.

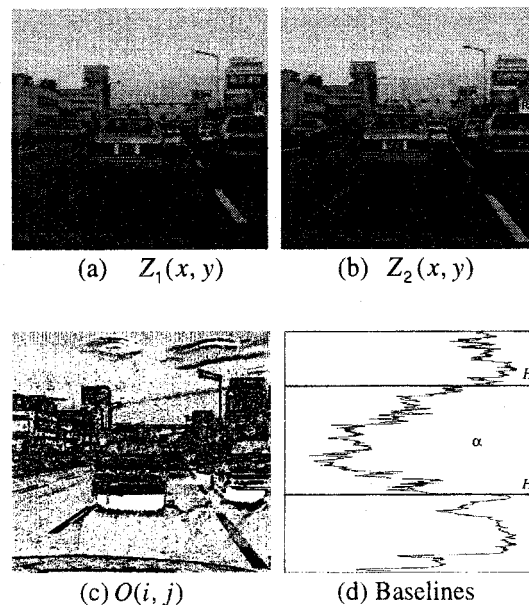


Fig. 1: XOR operation on two successive images

### 2.2 Validation Region

We define a validation region as the region with relatively uniform intensity distribution. We provide a constraint for the construction of a validation region  $\Omega$  not to contain the rear windscreen which has very strong specula property. It does not show a homogeneous property with respect to intensity distribution. Constructing a validation region  $\Omega$  satisfying the constraint is difficult. Therefore, we set a constant  $\xi$  experimentally and determine the validation region as  $H_r - \xi \leq \Omega \leq H_s$ . Fig. 2 shows the experimental basis for constructing an  $\Omega$ . While the intensity profiles of rows 207, 223 and 237 shown in Fig. 2 do not show a similar part, the intensity profiles of rows 272, 284 and 300 shown in Fig. 2 present a uniform intensity distribution on the part corresponding to the vehicle of interest. Accordingly, a validation region  $\Omega$  is constructed on this area.

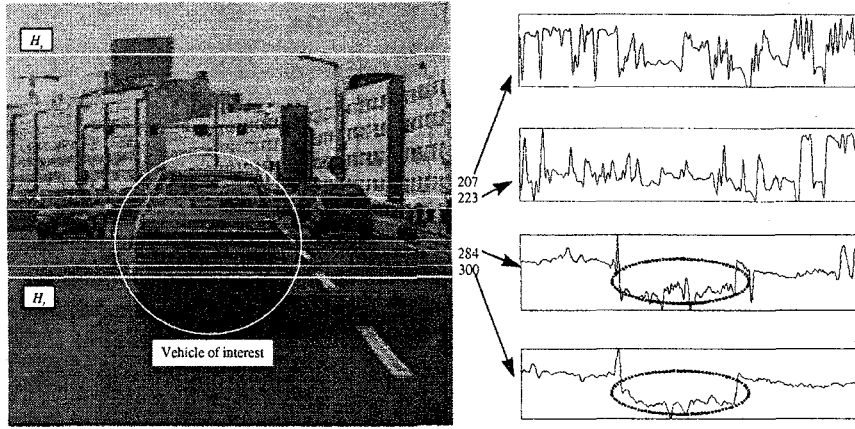


Fig. 2: An image and its intensity distribution along a horizontal direction

### 2.3 Extraction of Features for Evidential Reasoning

#### 2.3.1 Local Symmetry of an Intensity Profile

Let be the average intensity distribution in the horizontal direction of a validation region  $\Omega$  as:

$$f(i) = \sum_{j \in \Omega} Z_2(i, j) / \xi, \quad 0 \leq i < d \quad (2)$$

We take into account the column width of an image as an evaluation interval  $d$ . Using the substitution  $x = i - x_s$ , we can shift the origin of  $f(x)$  to any position  $x_s$  in the validation region along the horizontal direction. A parameter  $w$  will be used for varying the size of interval being evaluated and the parameter  $x_s$  may be thought of as denoting the location of a potential symmetry axis with  $w$  being the width of the symmetric interval. We define the even signal and odd signal of  $f(x_s + x)$  for a given interval of width  $w$  about  $x_s$  such that

$$f_e(x_s + x) = \begin{cases} (f(i) + f(-i))/2, & \text{if } -w/2 \leq i \leq w/2 \\ 0, & \text{otherwise} \end{cases} \quad \text{and}$$

$$f_o(x_s + x) = \begin{cases} (f(i) - f(-i))/2, & \text{if } -w/2 \leq i \leq w/2 \\ 0, & \text{otherwise} \end{cases}$$

The symmetry measure  $S(x_s, w)$  representing the degree of symmetry for any potential symmetry axis  $x_s$  with respect to an evaluating interval of width  $w$  is defined as:

$$S(x_s, w) = \frac{\int f_e^n(x_s + x)^2 dx - \int f_o(x_s + x)^2 dx}{\int f_e^n(x_s + x)^2 dx + \int f_o(x_s + x)^2 dx}, \quad (3)$$

$$-1 \leq S(x_s, w) \leq 1$$

where  $f_e^n(x_s + x) = f_e(x_s + x) - \frac{1}{w} \int_{-w/2}^{w/2} f_e(x_s + x) dx$ .

As a confidence measure to fathom the significance of  $x_s$  in an interval of width  $w$ , we use  $S_c(x_s, w, w_{max})$  defined by Zielk *et al.* [5] as follows:

$$S_c(x_s, w, w_{max}) = \frac{w}{2w_{max}} (S(x_s, w) + 1), \quad w \leq w_{max} \quad \text{and} \quad (4)$$

$$0 \leq S_c(x_s, w, w_{max}) \leq 1$$

where  $w_{max}$  is the maximal size of the symmetric interval.

Finding the local maxima from a symmetry measure as the hypotheses for symmetry axes of vehicles is carried out. First, we establish a set  $\Gamma_1$  with points that intersect  $S(x_s, w) = 0$  at the range of  $[0, \dots, d]$  as  $\Gamma_1 = \{x_k | S(x_k, w) = 0\}$ ,  $k = 1, 2, \dots, n$ . Second, we compute the length of  $l_j = x_{2j} - x_j$ ,  $j = 1, \dots, n/2$ , where  $x_{2j} \in \Gamma_1$  and  $x_j \in \Gamma_1$ . Finally, we construct the set of local maximum points with maximum values of  $S(x_s, w)$  within the range of respective  $l_j$  as follows:

$$\Gamma_2 = \{\hat{x}_p | S(\hat{x}_p, w) \geq S(x, w), \hat{x}_p \in l_j \text{ and } x \in l_j\}, \quad (5)$$

$$p = j = 1, \dots, n/2$$

#### 2.3.2 Gradient of Cumulative XOR Signal

We take a summation of the XOR signal of Eq. (1) for a validation region  $\Omega$  along the horizontal direction as  $u_i = \sum_{j \in \Omega} O(i, j)$ . To extract the gradient of  $u_i$ , we define

an one dimensional gradient filter  $T$  as shown in Fig. 3 and carry out the convolution of the filter  $T$  and  $u_i$  as:

$$H_{O_i} = T \otimes u$$

$$= -u_{i-4} - 2u_{i-3} - 3u_{i-2} - u_{i-1} + u_{i+1} + 3u_{i+2} + 2u_{i+3} + u_{i+4}$$

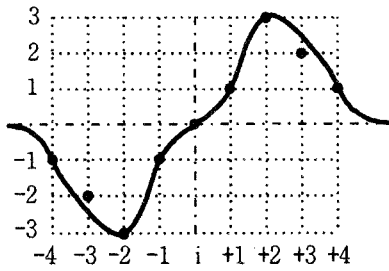


**Fig. 3:** An one-dimensional gradient filter

According to the fact that the strong discontinuities of the cumulative XOR signal in a validation region along the horizontal direction may usually correspond to a vehicle boundary, we find the local maxima of the profile of gradient magnitude  $|H_{O_i}|$  using the local maxima finding algorithm shown in Fig. 4. We utilize the algorithm with the mean and variance of  $|H_{O_i}|$  and let the set  $\mathfrak{R}_2$  obtained from Eq. (6) as  $\mathfrak{R}_O$ .

**Input :** gradient magnitude  $\nabla h_i$ , mean  $\mu$  and variance  $\sigma^2$  of the subject of consideration

- 1) Compute a reference line  $\beta = \mu + \lambda \cdot \sigma$  in which  $\lambda$  is Gaussian constant satisfying the predetermined confidence level.
- 2) Construct a set  $\mathfrak{R}_1 = \{i | \arg(\Delta h_i = \beta)\}$  and if first element  $\nabla h_1$  is greater than  $\beta$  discard the first element of  $\mathfrak{R}_1$ .
- 3) Let  $n = \|\mathfrak{R}_1\|$ . If  $n < 2$  then adjust  $\lambda$  and goto 1).
- 4) Make  $\mathfrak{R}_1$  to ascending order and obtain the length  $l_k = i_{2k} - i_k, k = 1, \dots, n/2$ . Then, construct a set  $\mathfrak{R}_2$  as:

$$\mathfrak{R}_2 = \left\{ i_k^* \mid \Delta h_{i_k^*} > \Delta h_{i_k}, i_k^* \in l_k \text{ and } i \in l_k, k = 1, 2, \dots, n/2 \right\}$$

(6)  
**Output :** Set  $\mathfrak{R}_2$  of locations of local maxima

**Fig. 4:** Local maxima finding algorithm

### 2.3.3 Gradient of Intensity Distribution

We take the convolution of the filter  $T$  defined in Fig. 3 to the mean intensity distribution  $f_i$  of Eq. (2) along the horizontal direction as follows:

$$H_{I_i} = T \otimes f$$

$$= -f_{i-4} - 2f_{i-3} - 3f_{i-2} - f_{i-1} + f_{i+1} + 3f_{i+2} + 2f_{i+3} + f_{i+4}$$

and find the local maxima of mean intensity profile  $|H_{I_i}|$  using the algorithm defined in Fig. 4 and let the set  $\mathfrak{R}_2$  obtained from Eq. (6) as  $\mathfrak{R}_I$ .

### 2.3.4 Cumulative Vertical Edge

We obtain the sum of vertical edge component for each column position in a validation region along the horizontal direction as follows:

$$H_{E_i} = \sum_{j \in \Omega} |G(i, j)|$$

$$G(i, j) = (Z(i+1, j-1) + 2Z(i+1, j) + Z(i+1, j+1)) - (Z(i-1, j-1) + 2Z(i-1, j) + Z(i-1, j+1))$$

Since the strong discontinuities on the profile of  $H_{E_i}$  may correspond to the outmost lines of a vehicle, we also find the local maxima of cumulative edge profile  $H_{E_i}$  using the algorithm in Fig. 4 and let the set  $\mathfrak{R}_2$  obtained from Eq. (6) as  $\mathfrak{R}_E$ .

We illustrate the local maxima finding results for the gradient of cumulative XOR signal (in Fig.5(a)), the gradient of mean intensity profile (in Fig.5(b)) and the cumulative vertical edge profile (in Fig.5(c)).

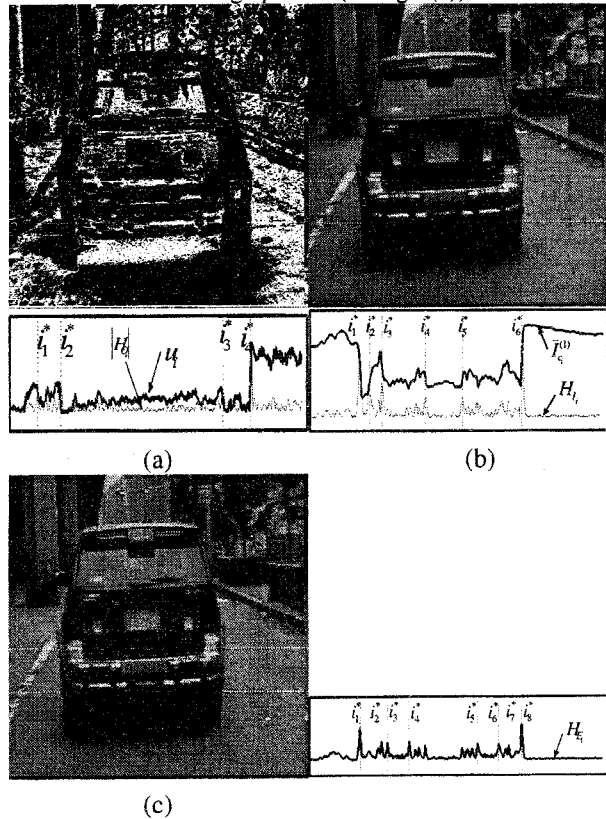


**Fig. 5:** Illustration of local maxima

#### 2.4 Evidential Reasoning by MAP Probability

Basically, the criteria underlying the evidential reasoning for a vehicle in an image are classified into 1) a true symmetric axis is insensitive to a little shifting a validation region along vertical direction, 2) a true symmetric axis has the strong vertical edge components on both sides of itself, 3) a true symmetric axis has the strong discontinuities in intensity distribution on both sides of itself, 4) a true symmetric axis lies on the area where strong horizontal edge components exist a lot. We describe the evidential reasoning for a vehicle in an image by MAP probability evaluating the closeness of the position of an extracted potential symmetric axis to its true position.

##### 2.4.1 Prior Probability

Since the prior probability  $p(\theta)$  means that a symmetric axis is likely to be present in an image  $Z$ , we consider  $p(\theta)$  as the confidence measure of a symmetric axis  $\hat{x}$  in  $\Gamma_2$  of Eq. (5), that is,

$$p(\theta) = S_c(\hat{x}, w, w_{\max}). \quad (7)$$

##### 2.4.2 Likelihood Probability

The likelihood probability  $p(\mathbf{z}|\theta)$  represents the probability of image feature  $\mathbf{z}$ , given a parameter  $\theta$ . We design the likelihood probability to have maximum value when the four criteria exactly match.

##### (1) Insensitivity from shifting a validation region

First, we shift a validation region  $\Omega$  to  $\Omega'$  as much as  $\Delta$  along vertical direction and obtain the set  $\Gamma_3$  of new hypotheses of extracted symmetric axes using the proposed algorithm in section 2.3.1. Second, we compute the distance for a symmetric axis  $\hat{x}$  in  $\Gamma_2$  of Eq. (5) against all symmetric axes in  $\Gamma_3$  as  $\delta_j = |\hat{x} - \hat{x}_j|$ ,  $\hat{x}_j \in \Gamma_3$ ,  $j = 1, \dots, q$ . Third, we define a characteristic function  $g_1$  as  $g_1 = \min(\delta_j)$ ,  $j = 1, 2, \dots, q$ .

##### (2) Symmetric degree of local maxima of the gradient of intensity distribution

First, we divide the set  $\mathfrak{R}_I$  obtained in section 2.3.3 into two sets for a symmetric axis  $\hat{x}$  in  $\Gamma_2$  as

$$\mathfrak{R}_I^{(L)} = \{i_k | i_k < \hat{x}, i_k \in \mathfrak{R}_I, k = 1, \dots, p\} \text{ and}$$

$$\mathfrak{R}_I^{(R)} = \{j_l | j_l > \hat{x}, j_l \in \mathfrak{R}_I, l = 1, \dots, q\}.$$

Second, we compute the absolute distances for each element in  $\mathfrak{R}_I^{(L)}$  and  $\mathfrak{R}_I^{(R)}$  against  $\hat{x}$  as  $\delta_k = |i_k - \hat{x}|$ ,  $i_k \in \mathfrak{R}_I^{(L)}$  and  $\delta_l = |j_l - \hat{x}|$ ,  $j_l \in \mathfrak{R}_I^{(R)}$ . Third,

we define a characteristic function  $g_2$  as  $g_2 = \min(\delta_{kl})$ , where  $\delta_{kl} = |\delta_k - \delta_l|$ ,  $k = 1, \dots, p$ ,  $l = 1, \dots, q$ . If  $\mathfrak{R}_I^{(L)} = \{\phi\}$  or  $\mathfrak{R}_I^{(R)} = \{\phi\}$ , we consider  $g_2 = \infty$ .

##### (3) Symmetric degree of local maxima of cumulative vertical edge

First, we divide the set  $\mathfrak{R}_E$  obtained in section 2.3.4 into two sets for a symmetric axis  $\hat{x}$  in  $\Gamma_2$  as:

$$\mathfrak{R}_E^{(L)} = \{i_k | i_k < \hat{x}, i_k \in \mathfrak{R}_E, k = 1, \dots, p\} \text{ and}$$

$$\mathfrak{R}_E^{(R)} = \{j_l | j_l > \hat{x}, j_l \in \mathfrak{R}_E, l = 1, \dots, q\}.$$

Second, we compute the absolute distances for each element in  $\mathfrak{R}_E^{(L)}$  and  $\mathfrak{R}_E^{(R)}$  against  $\hat{x}$  as  $\delta_k = |i_k - \hat{x}|$ ,  $i_k \in \mathfrak{R}_E^{(L)}$  and  $\delta_l = |j_l - \hat{x}|$ ,  $j_l \in \mathfrak{R}_E^{(R)}$ . Third, we define a characteristic function  $g_3$  as  $g_3 = \min(\delta_{kl})$ , where  $\delta_{kl} = |\delta_k - \delta_l|$ ,  $k = 1, \dots, p$ ,  $l = 1, \dots, q$ . If  $\mathfrak{R}_E^{(L)} = \{\phi\}$  or  $\mathfrak{R}_E^{(R)} = \{\phi\}$ , we consider  $g_3 = \infty$ .

##### (4) Horizontal edge component

First, we obtain the sum of horizontal edge component for each column position in a validation region  $\Omega$  along the horizontal direction as follows:

$$V_{E_i} = \sum_{j \in \Omega} |G(i, j)|,$$

$$G(i, j) = (Z(i-1, j+1) + 2Z(i, j+1) + Z(i+1, j+1)) - (Z(i-1, j-1) + 2Z(i, j-1) + Z(i+1, j-1)).$$

Then, we define the characteristic function  $g_4$  for a symmetric axis  $\hat{x}$  in  $\Gamma_2$  as

$$g_4 = \begin{cases} 0 & \text{if } V_{E_i} \geq \mu \\ \mu - V_{E_i} & \text{otherwise} \end{cases}$$

where  $\mu = \sum_i V_{E_i} / N$ ,  $N$  is number of column pixels.

##### (5) Likelihood probability

Consequently, the likelihood probability  $p(\mathbf{z}|\theta)$  is defined as the energy minimization problem modeled by:

$$p(\mathbf{z}|\theta) = \exp\left\{-\frac{1}{\kappa}(g_1 + g_2 + g_3 + g_4)\right\} \quad (8)$$

where  $\kappa$  is a normalization coefficient and  $g_1, g_2, g_3$  and  $g_4$  are characteristic functions.

##### 2.4.3 Posterior Probability

Using Bayes rule, we can write the posterior probability  $p(\theta|\mathbf{z})$  as

$$p(\theta|\mathbf{z}) = \frac{p(\mathbf{z}|\theta)p(\theta)}{p(\mathbf{z})}. \quad (9)$$

Since  $p(\mathbf{z})$  does not depend on  $\theta$ , the MAP estimator maximizes  $p(\mathbf{z}|\theta)p(\theta)$ . In the long run,  $p(\mathbf{z}|\theta)p(\theta)$

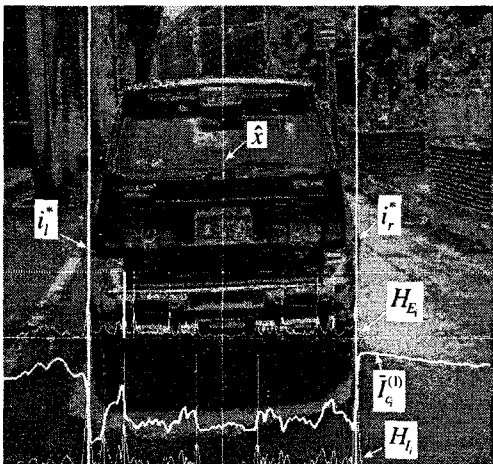
evaluates whether a symmetric axis  $\hat{x}$  in  $\Gamma_2$  is close to a true axis of a vehicle or not. We construct a set  $\Gamma$  as follows:

$$\Gamma = \{ \hat{x} | p(z|\hat{x})p(\hat{x}) > \varphi, \hat{x} \in \Gamma_2 \} \quad (10)$$

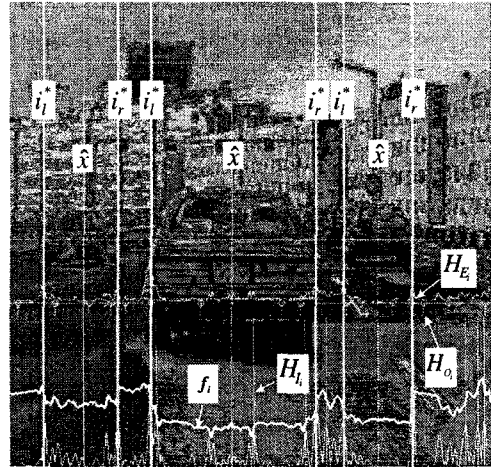
where  $p(z|\hat{x})p(\hat{x})$  is the MAP estimator of  $p(\hat{x}|z)$  and  $\varphi$  is a threshold.

### 2.5 Extraction of Vehicle Width

The basic idea underlying the extraction of a vehicle width is that the local maxima of cumulative vertical edge may be coincided with the local maxima of the gradient of mean intensive profile at the vicinity of vehicle boundary. The Extraction of a vehicle width is carried out by finding the coinciding positions of the both local maxima satisfying symmetric degree for a symmetric axis  $\hat{x}$  in  $\Gamma$  of Eq. (10). Since the local maxima of the gradient of cumulative XOR signal normally corresponds to the motion boundary of a rigid body, we use them as the supplementary measures in extracting a vehicle width. We illustrate an example of the extraction of a vehicle width in Fig. 6 in which  $\hat{x}$  represents a symmetric axis in  $\Gamma$  of Eq. (10),  $i_l^*$  and  $i_r^*$  represent the left and right outermost lines of a vehicle,  $f_i$  represents a mean intensity profile, and  $H_E$ ,  $H_{I_i}$  and  $H_O$  represent the local maxima of cumulative vertical edge and the gradients of mean intensity profile and cumulative XOR signal, respectively.



(a) Single vehicle



(b) Multiple vehicles

Fig. 6: Finding the left and right outermost lines of vehicles

### 3: Conclusion

We newly proposed an evidential reasoning-based object segmentation method capable of extracting vehicles in an outdoor natural scene. This method overcomes the limitations from several previous methods such as the model-based method and motion-based method. Proposed MAP-based probabilistic approach was insensitive to noise sources from a dynamic and complex scene and gave rise to precise categorical extraction of vehicles.

### References

- [1] M.P. Dubuisson, S. Lakshmanan, and A.K. Jain, Vehicle Segmentation and Classification Using Deformable Templates, *IEEE Trans. Pattern Anal. Mach. Intell.*, Vol.18, No.3, pp.293-308, 1996.
- [2] S.M. Smith and J.M. Brady, ASSET-2: Real time motion segmentation and shape tracking, *IEEE Trans. Pattern Anal. Mach. Intell.*, Vol. 17, No.8, pp.814-820,1995.
- [3] D. Koller, K. Daniilidis and H.H. Nagel, Model-Based Object Tracking in Monocular Image Sequences of Road Traffic Scenes, *IJCV*, Vol. 10, No.3, pp.257-281, 1993.
- [4] M. Xie, L. Trassoudaine, J. Alizon, and J. Gallice, Road Obstacle Detection and Tracking by an Active and Intelligent Sensing Strategy, *Machine Vision and Applications*, Vol. 7, pp.165-177, 1994
- [5] T. Zielke, M. Brauckmann and W. V. Seelen, Intensity and Edge-Based Symmetry Detection with an Application to Car-Following, *CVGIP:Image Understanding*, Vol.58, No.2, pp.177-190, 1993.